ACS APPLIED MATERIALS & INTERFACES

Research Article

Cite This: ACS Appl. Mater. Interfaces 2018, 10, 4113−4120

www.acsami.org

New Insights into the Compositional Dependence of Li-Ion Transport in Polymer−Ceramic Composite Electrolytes

Jin Zheng[†] and Yan-Yan Hu*[,†,‡]

[†]Department of Chemistry and Biochemistry, Florida State University, Tallahassee, Florida 32306, United States

[‡]Center of Interdisciplinary Magnetic Resonance, National High Magnetic Field Laboratory, Tallahassee, Florida 32310, United States

Supporting Information

ABSTRACT: Composite electrolytes are widely studied for their potential in realizing improved ionic conductivity and electrochemical stability. Understanding the complex mechanisms of ion transport within composites is critical for effectively designing high-performance solid electrolytes. This study examines the compositional dependence of the three determining factors for ionic conductivity, including ion mobility, ion transport pathways, and active ion concentration. The results show that with increase in the fraction of ceramic $Li_7La_3Zr_2O_{12}$ (LLZO) phase in the LLZO−poly(ethylene oxide) composites, ion mobility decreases, ion transport pathways transit from polymer to ceramic routes, and the active ion concentration increases. These changes in ion mobility, transport pathways, and concentration collectively explain the observed trend of ionic conductivity in composite electrolytes. Liquid additives alter ion transport pathways and increase ion mobility, thus enhancing ionic conductivity significantly. It is also found that a higher content of LLZO leads to improved electrochemical stability of composite electrolytes. This study provides insight into the recurring observations of compositional dependence of ionic conductivity in current composite electrolytes and pinpoints the intrinsic limitations of composite electrolytes in achieving fast ion conduction.

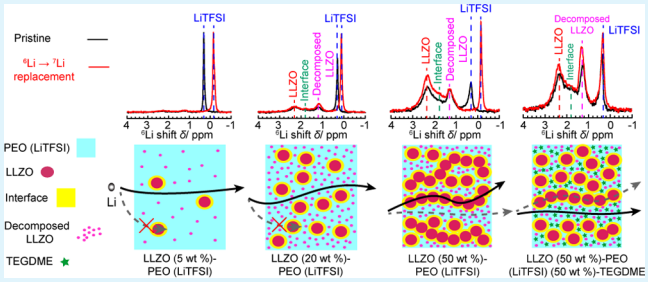

KEYWORDS: *Li-ion transport, composite electrolyte, isotope replacement, NMR, solid-state batteries*

INTRODUCTION

The current generation of rechargeable Li-ion batteries (LIBs) employs liquid electrolytes, which are toxic, flammable, and corrosive, resulting in significant safety issues.[1−4] To address these safety issues, in addition to improving the energy density of rechargeable LIBs, solid electrolytes are considered a promising solution. There are two major types of solid electrolytes: inorganics (ceramics and glasses) and polymers.[5−7]

Inorganic oxides, such as $Li_7La_3Zr_2O_{12}$ (LLZO), $Li_{3x}La_{2/3-x}TiO_3$ (LLTO), and $Li_{1+x}Al_xGe_{2-x}(PO_4)_3$ (LAGP), have been widely studied. The ionic conductivity is around 10^{-4} S/cm at room temperature (RT).[8−10] Ceramic electrolytes are often rigid and brittle with low flexibility, which leads to poor contact and high resistance at the electrolyte−electrode interfaces.[11,12] Polymers are flexible and show good contact with electrodes.[13−15] The widely studied polymers, poly(ethylene oxide) (PEO), polyacrylonitrile (PAN), and poly(methyl methacrylate), show a low conductivity of 10^{-5}−10^{-8} S/cm at RT. In addition, polymers exhibit poor thermal and chemical stabilities.[16−18]

To mitigate the shortcomings of pure polymer or ceramic electrolytes, the potential composite electrolytes have been explored extensively.[19] In the early studies, nonconductive oxides, such as Al_2O_3, TiO_2, and SiO_2, were dispersed into polymer matrix to prepare composite electrolytes. The increase of conductivity by 2 orders of magnitude was obtained compared with that of pure polymer electrolytes.[20,21] The ionic conductivity enhancement is attributed to suppression of polymer crystallization. The amorphous phase of polymers with active chain segments is believed to promote fast Li-ion transportation.[22] Generally, the optimal insulating filler concentration for ionic conductivity is about 10 wt %. Further increase in the fraction of fillers results in a conductivity decrease due to dilution and block effects.[23,24] To overcome the limitation of conventional composite electrolytes with insulating ceramic fillers, a few research groups have investigated hybrid materials made of polymers and Li-ion conductive ceramics or glasses.[25−27] In these cases, the optimal fraction of active fillers varied in a large range. For example, in nanowire LLTO−PAN composite electrolytes, the highest conductivity was obtained at 15 wt %.[28] However, for LAGP−PEO composite electrolytes, the highest conductivity at RT was achieved at 80 wt % of LAGP.[29] In these composite systems, Li ions can transport via the polymer matrix, inorganic fillers, the organic−inorganic interfaces, or a combination of the three. Li-ion transport pathways, together with active Li-ion concentration and Li-ion mobility, determine the ionic conductivity of Li electrolytes. Thus, exploring the mechanism of Li-ion

Received: November 13, 2017
Accepted: January 5, 2018
Published: January 5, 2018

DOI: 10.1021/acsami.7b17301
ACS Appl. Mater. Interfaces 2018, 10, 4113−4120

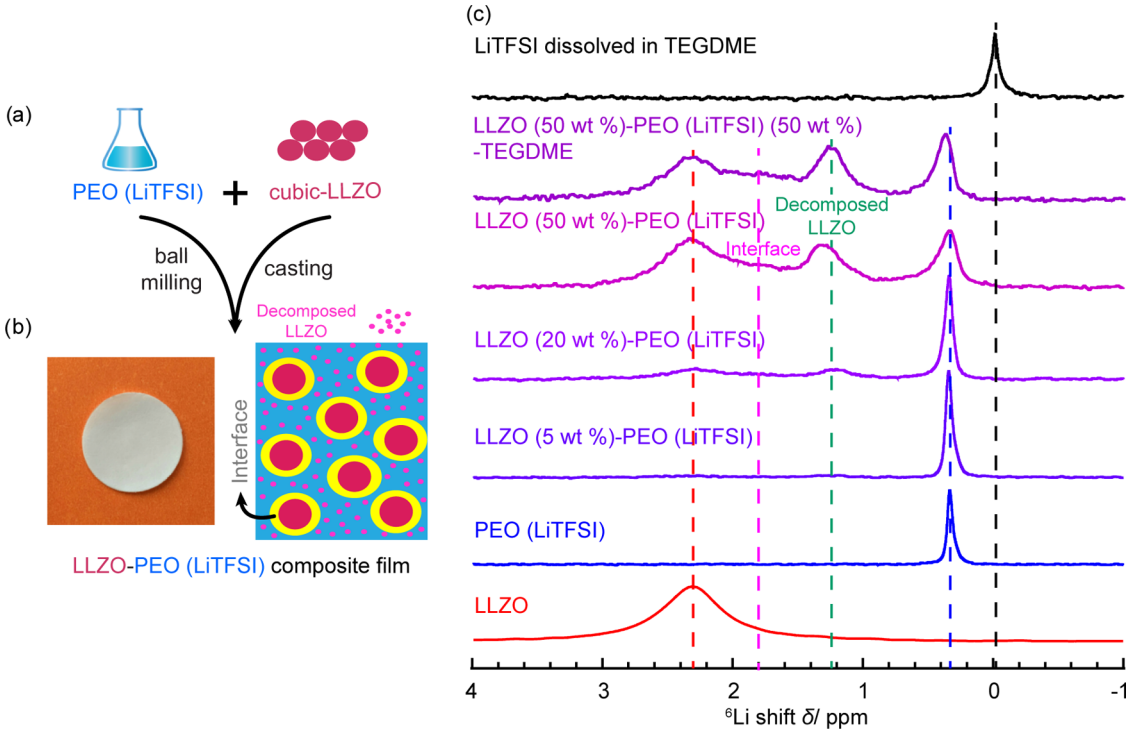

Figure 1. (a) Illustration of the preparation process of LLZO−PEO (LiTFSI) composite electrolytes. (b) Appearance and schematic diagram of the composite film. (c) ^{6}Li MAS NMR spectra of LLZO, PEO (LiTFSI), LLZO (5 wt %)−PEO (LiTFSI), LLZO (20 wt %)−PEO (LiTFSI), LLZO (50 wt %)−PEO (LiTFSI), and LLZO (50 wt %)−PEO (LiTFSI) (50 wt %)−TEGDME.

transportation is crucial but challenging. To study the local structural environments and dynamics of Li ions, solid-state NMR has proved to be a powerful tool.[30−32] In this contribution, Li-ion transport pathways within a series of polymer−ceramic composite electrolytes are identified. In addition, the relative effects of ion transport pathways, ion mobility, and active Li concentration on ionic conductivity are determined.

EXPERIMENTAL SECTION

Synthesis of Cubic-$Li_7La_3Zr_2O_{12}$ (LLZO). Precursors of cubic LLZO were prepared with a sol−gel method using citric acid as organic complexing agent. LiOH (Sigma-Aldrich), $La(NO_3)_3{\cdot}6H_2O$ (Alfa Aesar), $Zr(OC_4H_9)_4$ (Sigma-Aldrich, 80 wt % in 1-butanal), $Al(NO_3)_3{\cdot}9H_2O$ (Alfa Aesar), and citric acid (Sigma-Aldrich) with the molar ratio of 8.4:3.0:2.0:0.2:5.0 were dissolved in dilute HNO_3. Excess LiOH (20 wt %) was added to compensate for the evaporation of Li during high-temperature sintering. Al was added to stabilize cubic LLZO. The solution was stirred at 80 °C overnight to form a homogeneous gel and dried at 200 °C for 2 h. The dry powders were sintered at 290 °C for 2 h and 900 °C for 8 h. The scanning electron microscopy (SEM) images of LLZO powders are shown in Figure S1. The size of LLZO particles ranges from 5 to 20 μm.

Preparation of Composite Films. All composite films were prepared by a solution casting method. The polymer matrix was made by dissolving poly(ethylene oxide) (PEO) (Sigma-Aldrich, Mw: 400 000) and lithium bis(trifluoromethanesulfonyl)imide (LiTFSI) (Sigma-Aldrich) in anhydrous acetonitrile. The ratio of [EO]/[Li] was fixed at 18:1. LLZO was added into the PEO (LiTFSI), and the mixture was ball-milled at 200 rpm for 4 h. Then, the slurry was cast on a flat Teflon plate and dried in an argon-filled glovebox for 12 h. The composite films with different fractions of LLZO, from 5 to 20 and 50 wt %, were made. The thickness was around 30−50 μm. In addition, tetraethylene glycol dimethyl ether (TEGDME) (Sigma-Aldrich) was dissolved in the PEO (LiTFSI) solution and then mixed with LLZO with ball-milling to prepare LLZO (50 wt %)−PEO (LiTFSI) (50 wt %)−TEGDME composite electrolyte. TEGDME accounts for 20 wt % of the composite.

Electrochemical Measurements. The conductivity of composite films was determined with electrochemical impedance spectroscopy (EIS). The composite film was sandwiched between two Li electrodes. Alternating current impedance measurements were performed with a Gamry Reference 600+ over the frequency range of 5 MHz to 1 Hz. Galvanostatic cycling of the symmetric battery cells was carried out on a LANHE (CT2001A) battery testing system, with a constant current density of 15 μA/cm^2. For ^{6}Li → ^{7}Li replacement, ^{6}Li metal foils were used as the two electrodes.

Solid-State NMR. ^{6}Li magic-angle spinning (MAS) NMR experiments were performed on a Bruker Avance III-500 spectrometer with a 2.5 mm Bruker HXY triple-resonance probe. The sample was spun at 25 kHz, and the spectra were collected at the ^{6}Li Larmor frequency of 73.6 MHz. LiCl with the ^{6,7}Li shift at 0 ppm was used as a reference.

RESULTS AND DISCUSSION

Ionic conductivity (σ) of Li electrolytes is determined by $\sigma = ne\mu$, where n is the concentration of conducting Li ions, e is the unit charge, and μ is Li-ion diffusivity. μ is largely affected by Li-ion mobility and transport pathways. In this study, LLZO−PEO (LiTFSI) composites with various LLZO contents are prepared, and Li-ion transport pathways in these composites are determined by a ^{6}Li → ^{7}Li isotope replacement method. With the determination of Li transport pathways, the participating Li ions in the conduction process are identified and quantified on the basis of the NMR spectra. NMR relaxation time measurements are performed to probe variations in Li-ion mobility of LLZO−PEO (LiTFSI) composites. The ionic conductivity of LLZO−PEO (LiTFSI) composites with various LLZO contents is determined with electrochemical impedance spectroscopy (EIS). The respective contribution of ion transport pathway, ion mobility, and active

DOI: 10.1021/acsami.7b17301
ACS Appl. Mater. Interfaces 2018, 10, 4113−4120

Table 1. ^{7}Li T_1 Results of PEO (LiTFSI), LLZO (5 wt %)−PEO (LiTFSI), LLZO (20 wt %)−PEO (LiTFSI), LLZO (50 wt %)−PEO (LiTFSI), and LLZO (50 wt %)−PEO (LiTFSI) (50 wt %)−TEGDME

T_1/s	PEO (LiTFSI)	LLZO (5 wt %)−PEO (LiTFSI)	LLZO (20 wt %)−PEO (LiTFSI)	LLZO (50 wt %)−PEO (LiTFSI)	LLZO (50 wt %)−PEO (LiTFSI) (50 wt %)−TEGDME
LiTFSI	0.28	0.35	0.52	0.73	0.69
LLZO and interface			0.75	1.33	1.18
decomposed LLZO			11.36	19.28	11.16

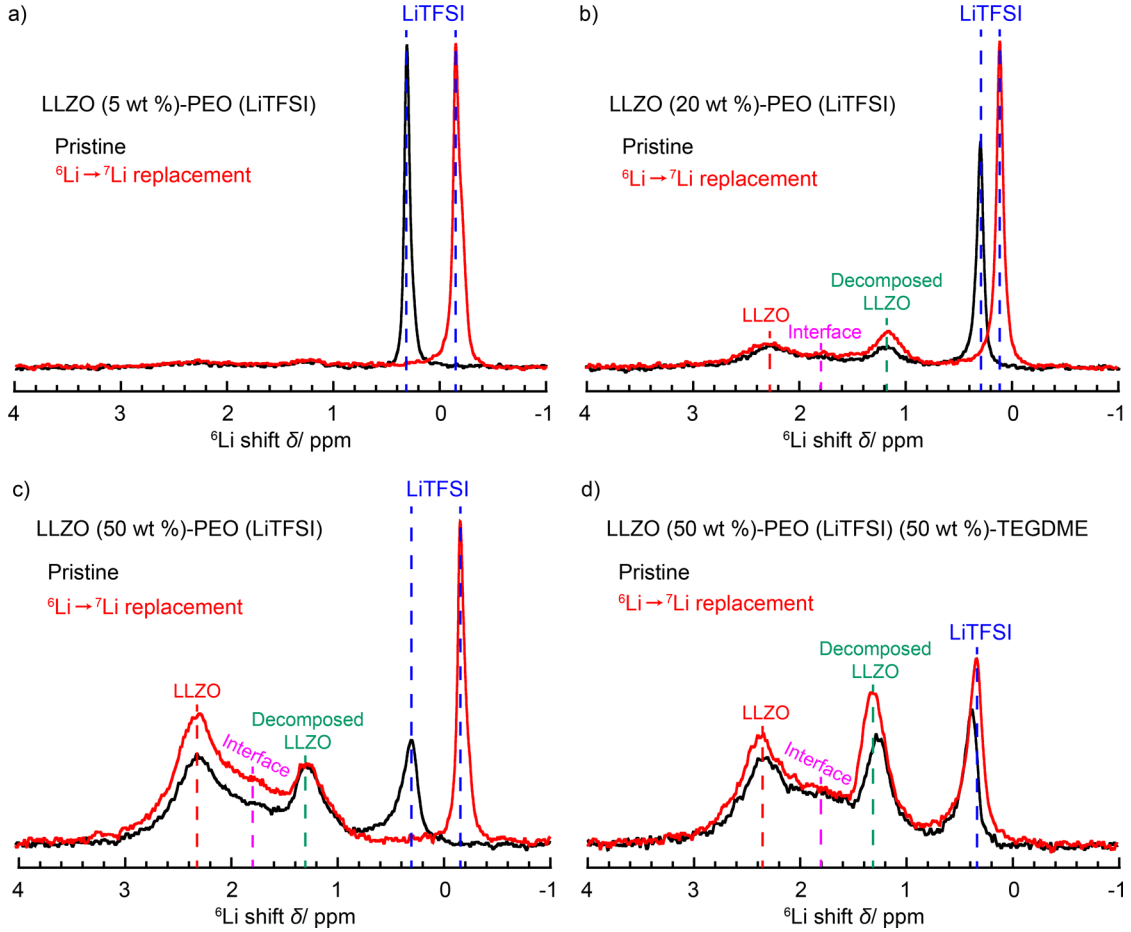

Figure 2. ^{6}Li NMR comparison of pristine and cycled LLZO (5 wt %)−PEO (LiTFSI), LLZO (20 wt %)−PEO (LiTFSI), LLZO (50 wt %)−PEO (LiTFSI), and LLZO (50 wt %)−PEO (LiTFSI) (50 wt %)−TEGDME.

Li concentration toward the measured ionic conductivity of LLZO−PEO (LiTFSI) composites is discussed.

The preparation process of composite electrolytes, as described in the Experimental Section, is illustrated in Figure 1a. A picture of the resulting flexible, white film made of LLZO−PEO (LiTFSI) and a schematic diagram of film composition are shown in Figure 1b. The thickness of composite films ranges from 30 to 50 μm. To characterize these composite electrolytes, high-resolution solid-state ^{6}Li MAS NMR was employed (Figure 1c). PEO (LiTFSI), pure cubic LLZO, and LiTFSI dissolved in TEGDME were used as references in the characterizations. Pure cubic LLZO, LiTFSI in PEO, and LiTFSI in TEGDME show ^{6}Li NMR peaks at 2.3, 0.3, and 0 ppm, respectively. The ^{6}Li NMR signal of LLZO at 2.3 ppm remains the same in all of the composite electrolytes of interest, except that the amount of LLZO is too small to be observed for LLZO (5 wt %)−PEO (LiTFSI). In the ^{6}Li NMR spectra of LLZO−PEO (LiTFSI) composites, a broad shoulder at 1.8 ppm is assigned to the LLZO−PEO interface, which was verified in our previous study.[30] A new peak at 1.3 ppm is from decomposed LLZO due to the ball-milling process during composite preparation. The decomposed LLZO is confirmed to be Li_2CO_3 with high-resolution ^{6}Li NMR (Figure S2). The intensity of the decomposed LLZO peak is increased when the liquid additive TEGDME is added, suggesting that TEGDME enhances the breakdown of LLZO. The NMR peak shifts slightly from 1.3 to 1.2 ppm, likely owing to change of the surrounding matrix of decomposed LLZO from PEO to PEO−TEGDME complex. It is also observed that the area integral of the interface signal at 1.8 ppm is increased with the addition of TEGDME, indicating that more bulk LLZO is converted to interface. More details about the effects of TEGDME are shown in Figure S3 and in our prior work.[32]

The participation of LLZO in the composite electrolytes broadens the signal of LiTFSI in PEO. The full-width-at half-maximum (FWHM) of the LiTFSI resonance in the PEO-only

DOI: 10.1021/acsami.7b17301
ACS Appl. Mater. Interfaces 2018, 10, 4113−4120

Table 2. Enhancement of ^{6}Li Amount in Each Component after Cycling for LLZO (5 wt %)−PEO (LiTFSI), LLZO (20 wt %)−PEO (LiTFSI), LLZO (50 wt %)−PEO (LiTFSI), and LLZO (50 wt %)−PEO (LiTFSI) (50 wt %)−TEGDME

increase/%	LLZO	interface	decomposed LLZO	LiTFSI
LLZO (5 wt %)−PEO (LiTFSI)				**23.2**
LLZO (20 wt %)−PEO (LiTFSI)	2.3	1.1	**10.6**	**21.2**
LLZO (50 wt %)−PEO (LiTFSI)	**27.2**	6.3	1.2	8.7
LLZO (50 wt %)−PEO (LiTFSI) (50 wt %)−TEGDME	**7.0**	1.2	**13.8**	**14.0**

electrolyte is 0.05 ppm, whereas it increases to 0.07 and 0.18 ppm in LLZO (20 wt %)−PEO (LiTFSI) and LLZO (50 wt %)−PEO (LiTFSI), respectively (Table S1). It has been established that the addition of ceramic fillers can reduce polymer crystallization,[22] which in turn increases the disorder of Li-ion local environments within polymers, manifested as broadened LiTFSI resonances in ^{6}Li NMR. A minor reduction in the FWHM of the LiTFSI resonance from 0.18 to 0.15 is seen with the addition TEGDME to the LLZO−PEO (LiTFSI) composite. It is expected that liquid TEGDME will enhance Li-ion motion, which partially averages out the environmental anisotropy and thus reduces the NMR line width.

To probe the Li-ion mobility in the composite electrolytes, the ^{7}Li T_1 relaxation times are measured for the LiTFSI and LLZO associated phases. The results are shown in Table 1. With the increase of the LLZO fraction in the composite, the ^{7}Li T_1 relaxation times increase for Li in LiTFSI, which suggests a slowdown of Li-ion motion. The possible reasons are: (i) LLZO particles make the composite rigid, which limits the motion of Li ions within the matrix; and (ii) big LLZO particles are blocking Li-ion transport channels within the polymer. Both factors will result in reduced ion conduction within the polymer phase. The T_1 relaxation times for LLZO-related phases, including LLZO, LLZO−PEO interface, and decomposed LLZO, increase with larger LLZO content. The T_1 for bulk c-LLZO at room temperature is ∼1 s, which is not expected to change significantly with increase in LLZO amount in the composite. It also has been determined in our prior studies that Li at the LLZO−PEO interface shares the same $T_1 \sim 1$ s as Li in bulk LLZO.[32] The variation in T_1 in the LLZO-related phases is mainly from the contribution of the decomposed LLZO phase, which exhibits very long T_1 in the LLZO−PEO (LiTFSI) composites, that is, 10−20 s (Table 1). The ^{7}Li T_1 of decomposed LLZO in LLZO (50 wt %)−PEO (LiTFSI) (50 wt %)−TEGDME is reduced compared to that in LLZO (50 wt %)−PEO (LiTFSI), suggesting increased Li motion in TEGDME. The results show that Li-ion mobility decreases with increasing LLZO content in the composite, and small molecule additives such as TEGDME render Li ions in the composite more mobile.

To investigate Li-ion transport pathways within the composite electrolytes, symmetric cells, ^{6}Li metal|composite electrolyte|^{6}Li metal, were fabricated. These symmetric cells were electrochemically cycled with a current density of 7.2 μA/cm^2, and the direction of the current was switched every 5 min. The natural abundance of the ^{6}Li isotope is only 7.6%, which is low compared to that of 92.4% for ^{7}Li. The slightly biased potential induced by the electric current drives ^{6}Li ions from one ^{6}Li-enriched metal electrode to pass through the composite electrolyte and reach the other ^{6}Li-enriched metal electrode. During this process, ^{6}Li ions partially replace ^{7}Li ions in the composite electrolytes. Therefore, the components comprising Li-ion transport pathways will be preferentially ^{6}Li-enriched with repeated electrochemical cycling. Quantitative evaluation of the change in ^{6}Li amount for each component within the composite electrolyte will reveal the preferred pathways for Li-ion transport.

The ^{6}Li NMR spectra of pristine composite electrolytes and those after ^{6}Li → ^{7}Li replacement are shown in Figure 2. The quantification of ^{6}Li enrichment based on spectral area integrals is documented in Table 2. For the LLZO (5 wt %)−PEO (LiTFSI) composite, ^{6}Li enrichment of 23.3% is observed for LiTFSI in PEO, suggesting that Li ions pass through the PEO matrix for conduction. In addition to the intensity increase (Figure 2a), the ^{6}Li resonance also shifts to the right, an indication of change in Li-ion local environments. Li ions associated with crystalline PEO often exhibit a ^{6}Li resonance at ∼0.3 ppm, and the resonance tends to shift to lower ppm for Li in amorphous PEO due to reduced PEO−Li interactions.[32] Therefore, the shift of the resonance after ^{6}Li → ^{7}Li replacement is a manifestation of weakened Li−PEO interaction; this often facilitates Li-ion conduction.

With the increase in LLZO content to 20 wt % in the composite, that is, LLZO (20 wt %)−PEO (LiTFSI), the ^{6}Li signals from LLZO, PEO−LLZO interface, decomposed LLZO, and LiTFSI can be distinctively observed. After the ^{6}Li → ^{7}Li replacement operation, LLZO and interface resonances do not show any notable changes, whereas the ^{6}Li amount in decomposed LLZO and LiTFSI increased by 10.6 and 21.2%, respectively. The preferred ^{6}Li enrichment of decomposed LLZO and LiTFSI implies that Li-ion conduction occurs via Li salts in PEO. Li salts are partially from LiTFSI dispersed in PEO and partially from decomposed LLZO. The ball-milling mixing breaks bulk LLZO into small granules, and these decomposed LLZO particles are distributed within PEO. The extraordinarily large T_1 (>10 s) of decomposed LLZO compared to that (∼1 s) of other Li-containing components in the composite electrolytes suggests that decomposed LLZO is spatially in a separate phase. The lack of ^{1}H−^{6}Li cross-polarization signal for decomposed LLZO infers very weak interactions between decomposed LLZO and the PEO matrix (Figure S4). The low strength of the interaction again favors fast Li-ion conduction. The lack of bulk LLZO participation in Li conduction in LLZO (20 wt %)−PEO (LiTFSI) composite is likely due to the low LLZO content, which does not allow the formation of a percolated network for Li to pass through. In summary, LLZO (20 wt %)−PEO (LiTFSI) is still a polymer electrolyte modified by LLZO as fillers, and its decomposed form serves as an additional Li source.

For LLZO (50 wt %)−PEO (LiTFSI) (Figure 2c), after ^{6}Li → ^{7}Li replacement, the ^{6}Li peak of bulk LLZO at 2.3 ppm is increased significantly by 27.2%. In addition, the PEO−LLZO interface and LiTFSI resonances show small ^{6}Li enrichment, 6.3 and 8.7%, respectively. No ^{6}Li enrichment is observed for the resonance from decomposed LLZO. Therefore, the majority of Li ions pass through the percolated network formed by LLZO particles and a small portion transport via LiTFSI in PEO. Decomposed LLZO plays a minor role in Li-

DOI: 10.1021/acsami.7b17301
ACS Appl. Mater. Interfaces 2018, 10, 4113−4120

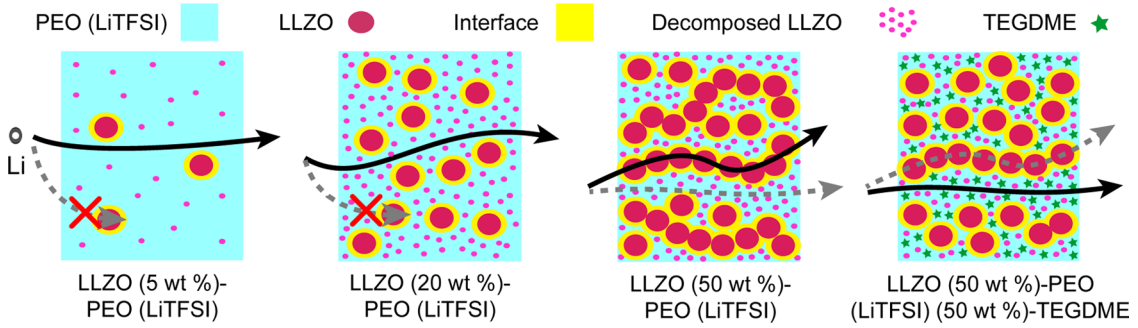

Figure 3. Schematic of Li-ion pathways within LLZO (5 wt %)−PEO (LiTFSI), LLZO (20 wt %)−PEO (LiTFSI), LLZO (50 wt %)−PEO (LiTFSI), and LLZO (50 wt %)−PEO (LiTFSI) (50 wt %)−TEGDME composite electrolytes.

ion conduction in LLZO (50 wt %)−PEO (LiTFSI), which is likely due to relatively high activation energies for Li-ion transport compared with other pathways. It is worth noting that in our previous study on LLZO (50 wt %)−PEO ($LiClO_4$) composite electrolyte, almost all Li ions transport through LLZO and few of them through $LiClO_4$ in PEO.[30] The difference of Li-ion transport pathways in LLZO (50 wt %)−PEO (LiTFSI) and LLZO (50 wt %)−PEO ($LiClO_4$) is precisely from the type of Li salts. In general, Li salts with bulkier anions exhibit higher ionic conductivity. For instance, the conductivity of PEO−$LiClO_4$ electrolytes is on the order of 10^{-7} S/cm at room temperature, whereas that of PEO−LiTFSI electrolytes is 10^{-5} S/cm. LiTFSI with larger anions can dissociate in the PEO matrix more easily and release more free Li ions than $LiClO_4$, resulting in significant conductivity enhancement. It is reported that, under similar stoichiometric Li concentrations, the measured free Li-ion concentration from LiTFSI in polymers is ∼3.4 times more than that from $LiClO_4$, which contributes to the observed much higher Li diffusivity of LiTFSI in polymers, ∼5.3 times more than that of $LiClO_4$.[33] From this perspective, it is not hard to understand that LiTFSI in PEO also makes measurable contribution to Li-ion transportation in the LLZO (50 wt %)−PEO (LiTFSI) composite electrolyte.

To further explore the influence of chemical environments on Li-ion pathways, a typical plasticizer, TEGDME, was added into LLZO−PEO (LiTFSI) during composite preparation. TEGDME has been used as a nonflammable liquid electrolyte for LIBs, and Li ionic conductivity of TEGDME is 10^{-3} S/cm at room temperature. TEGDME can also reduce PEO crystallization and increase the fraction of amorphous PEO phase, which is believed to account for fast Li-ion transport in PEO−TEGDME composites. It is seen in Figure 2d that the addition of TEGDME has altered Li-ion pathways compared with composites without TEGDME. Bulk LLZO is not the dominant component for Li-ion transportation anymore, showing only 7.0% ^{6}Li enrichment. The integrals of ^{6}Li resonances from decomposed LLZO and LiTFSI are increased by 14.8 and 14.0%, respectively. These results indicate that Li ions transport mainly through Li salts within the PEO−TEGDME matrix.

The schematic of Li-ion pathways within LLZO−PEO (LiTFSI) composite electrolytes of different LLZO contents is shown in Figure 3. To summarize, with low LLZO content (<20 wt %), LLZO−PEO (LiTFSI) composites behave as a polymer electrolyte modified by LLZO. On increasing LLZO amount to a critical point, LLZO particles connect to form a percolated network; thus, LLZO−PEO (LiTFSI) composites function as a ceramic electrolyte. However, the ceramic particles are diluted by polymers, and as a result, ceramic electrolytes composed of loose particles exhibit much lower ionic conductivity compared with dense ceramic pellets. Moreover, bulk LLZO particles block Li-ion transport through the polymer matrix. Li transport pathways transition from the PEO matrix to the percolated LLZO network when the LLZO fraction in the composite electrolyte is increased to a critical point. The exact transition point varies depending on many factors, including the particle size and morphology of LLZO as well as the mixing degree of participating components. With TEGDME additive, Li-ion conduction occurs mainly through TEGDME-modified polymer phase. The presence of TEGDME additive in PEO has been shown to significantly enhance Li-ion conduction.[34]

The determination of Li-ion transport pathways also permits the quantification of the relative concentration of active Li ions for conduction. For LLZO (5 wt %)−PEO (LiTFSI), the active Li ions are solely from LiTFSI. For LLZO (20 wt %)−PEO (LiTFSI), an additional source of active Li ions is the decomposed LLZO, which likely increases the charge carrier concentration and thus improves the ionic conductivity.[35] For LLZO (50 wt %)−PEO (LiTFSI), the main source of active Li ions is bulk LLZO, with a minor contribution from LiTFSI. For LLZO (50 wt %)−PEO (LiTFSI) (50 wt %)−TEGDME, active Li ions are from LiTFSI, decomposed LLZO, and bulk LLZO. It is worth pointing out that although the nominal amount of active Li ions increases with increasing LLZO content, the actual fraction of Li ions participating in the conduction may be reduced due to decreased ion mobility and blockage of pathways in PEO by LLZO particles, which we will discuss next.

The effects of increasing LLZO content in the LLZO−PEO (LiTFSI) composites on ionic conductivity channel through the following three avenues: (i) ion mobility: the T_1 relaxation time measurements suggest that increasing LLZO contents decrease ion mobility; (ii) ion transport pathways: ^{6}Li → ^{7}Li replacement experiments reveal that at a critical LLZO content, the composite will transition from a polymer electrolyte to a ceramic electrolyte; and (iii) concentration of participating Li ions in conduction: composites with <20 wt % LLZO show that the concentration of active Li ions rises with increasing LLZO content. With large LLZO content, on the one hand, the number of Li ions originated from LLZO increases. On the other hand, likely due to the blockage of Li conduction channels by LLZO particles, the amount of active Li ions in PEO is reduced. As is seen, LLZO content can have totally opposite effects on different parameters that determine ionic

DOI: 10.1021/acsami.7b17301
ACS Appl. Mater. Interfaces 2018, 10, 4113−4120

conductivity. On the basis of the above analysis, the qualitative evaluation of the impact of LLZO on ionic conductivity is as follows: at low content of LLZO (e.g., 5 wt %), LLZO serves as a filler to reduce the crystallinity of PEO. Large LLZO particles may also block the Li-ion pathways in PEO and reduce Li-ion mobility. Whether or not the fillers at a certain concentration enhance or reduce ionic conduction depends on the weighing of the two competing effects. In addition, if the filler contains Li, it may become an additional source of Li ions participating in conduction. For instance, in LLZO (20 wt %)−PEO (LiTFSI), Li from decomposed LLZO becomes one major charge carrier source, which is expected to enhance ionic conductivity. At high content of LLZO (e.g., 50 wt %), LLZO−PEO (LiTFSI) becomes an LLZO ceramic conductor. This is partially due to the formation of a percolated network of LLZO particles to make ion conduction within the LLZO matrix possible and partially due to the significant blockage of ion channels in PEO. Therefore, the ionic conductivity is largely determined by loosely connected LLZO particles, of which the ionic conductivity is on the order of 10^{-6}−10^{-7} S/cm (Figure S5). With the addition of a liquid additive such as TEGDME, the mobility of particles increases, which partially disintegrates the LLZO network. This has two effects: (i) Li-ion pathway through the LLZO network is largely broken, and the role of LLZO in ion conduction is reduced; (ii) it reduces the blockage of Li-ion channels in PEO. In addition, TEGDME further reduces PEO crystallinity and enhances ion mobility within the PEO−TEGDME complex. As a result, LLZO (50 wt %)−PEO (LiTFSI) (50 wt %)−TEGDME becomes predominantly a polymer electrolyte modified by a plasticizer.

The ionic conductivities of PEO and LLZO−PEO composite electrolytes with various fractions of LLZO and TEGDME are determined by EIS, with the results shown in Figure 4.

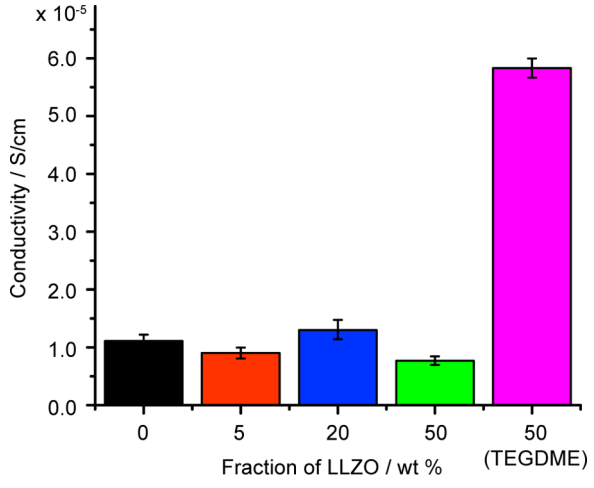

Figure 4. Conductivity of PEO (LiTFSI), LLZO (5 wt %)−PEO (LiTFSI), LLZO (20 wt %)−PEO (LiTFSI), LLZO (50 wt %)−PEO (LiTFSI), and LLZO (50 wt %)−PEO (LiTFSI) (50 wt %)−TEGDME.

Compared with PEO (LiTFSI), LLZO (5 wt %)−PEO (LiTFSI) showed a slight reduction in ionic conductivity. This suggests that blocking effect overweighs the benefits from reduced polymer crystallinity. About 1.5-fold conductivity enhancement is observed in LLZO (20 wt %)−PEO (LiTFSI); this is largely attributed to the increase in Li salt concentration from the decomposed LLZO (Figure 2 and Table 2). LLZO (50 wt %)−PEO (LiTFSI) shows notably lower ionic conductivity compared to that of other composites. This is due to the fact that LLZO particles almost completely block the pathways through PEO (Figure 2 and Table 2), and the alternative pathway through loosely connected LLZO particles does not provide high ionic conductivity. A significant enhancement in ionic conductivity is observed for LLZO (50 wt %)−PEO (LiTFSI) (50 wt %)−TEGDME due to increased ion mobility and re-established ion conduction channels within TEGDME-modified PEO.

The above discussion reveals various reasons accounting for the observations of changes in the ionic conductivities of composite electrolytes. Solid-state NMR is capable of clearly identifying the contributing factors, including ion mobility, ion transport pathways, and active ion concentration, and following their changes. This helps pinpoint why certain strategies for ionic conductivity enhancement fail and others work but for reasons other than apparent explanations. For instance, the observed increase in ionic conductivity for LLZO (20 wt %)−PEO (LiTFSI) is merely due to extra Li ions from decomposed LLZO, which has not been identified and discussed before. This may explain a number of observations in reported studies that large ionic conductivity was observed for Li-containing fillers compared to that for fillers without Li.[21−27] The results also infer that composites with a large content of ceramic particles in polymers are not likely to produce synergies for ionic conductivity enhancement, as the polymer−ceramic interfaces play a very small role in ion conduction.

Despite the fact that high content of LLZO does not lead to high ionic conductivity, it increases the stability of the composite when used in solid-state batteries with Li metal as the anode. Symmetric cells made of Li metal electrodes and PEO or composite electrolytes are cycled with a constant current of 15 μA/cm^2, and the current direction is switched every 60 min. The cell voltage profile as a function of cycling time is presented in Figure S6. The cell voltage increases over time for all electrolytes, indicating the increase of impedance induced by electrochemical instability. The voltage of PEO reached 10 V after 366 cycles. With the addition of LLZO, the stability improved significantly. LLZO (5 wt %)−PEO (LiTFSI) was cycled for 743 times before arriving at 10 V, and LLZO (50 wt %)−PEO (LiTFSI) lasted for 920 cycles before arriving at 5 V.

CONCLUSIONS

Ion conduction within composite electrolytes is very complex. As in single-component ion conductors, active ion concentration, mobility, and transport pathways determine ionic conductivity. The variations of these three parameters and their interplay within the multiple phases of composite electrolytes further complicate the mechanism for ion conduction. The study has employed solid-state NMR to determine ion mobility, ion transport pathways, and active concentration in LLZO−PEO composite electrolytes and their compositional dependence. The results have revealed that with increasing LLZO content, ion mobility decreases; ion transport pathways gradually transition from PEO phase to percolated network made of loosely connected LLZO particles; and the active Li-ion concentration increases in general but with certain loss due to LLZO-blocked pathways in the polymer phase. The compositional dependence of these three parameters explains the observed ionic conductivity in this work and also sheds light on many reported ionic conductivity measurements of

DOI: 10.1021/acsami.7b17301
ACS Appl. Mater. Interfaces 2018, 10, 4113−4120

composite electrolytes. In summary, this work demonstrates that the complicated ion conduction in composite electrolytes can be understood and solid-state NMR is a particularly useful tool for determining the contributing factors for ionic conduction. The methodology and results from this work will facilitate the development of high-performance composite electrolytes for rechargeable solid-state batteries.

■ ASSOCIATED CONTENT

Supporting Information

The Supporting Information is available free of charge on the ACS Publications website at DOI: 10.1021/acsami.7b17301.

Table of FWHM, SEM images, ^{6}Li NMR, ^{1}H−^{6}Li CP NMR, EIS, and electrochemical stability tests (PDF)

■ AUTHOR INFORMATION

Corresponding Author

*E-mail: hu@chem.fsu.edu.

ORCID

Jin Zheng: 0000-0003-1114-1135

Notes

The authors declare no competing financial interest.

■ ACKNOWLEDGMENTS

This study was sponsored by the NSF under Grant No. 1508404 and the Marion Milligan Mason Award, AAAS. All of the solid-state NMR experiments were carried out at the NHMFL, which is funded by the NSF under contract DMR-1157490.

■ REFERENCES

(1) Dunn, B.; Kamath, H.; Tarascon, J.-M. Electrical Energy Storage for the Grid: A Battery of Choices. *Science* **2011**, *334*, 928−935.

(2) Etacheri, V.; Marom, R.; Elazari, R.; Salitra, G.; Aurbach, D. Challenges in the Development of Advanced Li-Ion Batteries: A Review. *Energy Environ. Sci.* **2011**, *4*, 3243.

(3) Tarascon, J.-M.; Armand, M. Issues and Challenges Facing Rechargeable Lithium Batteries. *Nature* **2001**, *414*, 359−367.

(4) Dudney, N. J.; Li, J. Using All Energy in a Battery. *Science* **2015**, *347*, 131−132.

(5) Li, J.; Ma, C.; Chi, M.; Liang, C.; Dudney, N. J. Solid Electrolyte: The Key for High-Voltage Lithium Batteries. *Adv. Energy Mater.* **2015**, *5*, No. 1401408.

(6) Quartarone, E.; Mustarelli, P. Electrolytes for Solid-State Lithium Rechargeable Batteries: Recent Advances and Perspectives. *Chem. Soc. Rev.* **2011**, *40*, 2525.

(7) Manthiram, A.; Yu, X.; Wang, S. Lithium Battery Chemistries Enabled by Solid-State Electrolytes. *Nat. Rev. Mater.* **2017**, *2*, No. 16103.

(8) Meier, K.; Laino, T.; Curioni, A. Solid-State Electrolytes: Revealing the Mechanisms of Li-Ion Conduction in Tetragonal and Cubic LLZO by First-Principles Calculations. *J. Phys. Chem. C* **2014**, *118*, 6668−6679.

(9) Catti, M. First-Principles Modeling of Lithium Ordering in the LLTO ($Li_xLa_{2/3-X/3}TiO_3$) Superionic Conductor. *Chem. Mater.* **2007**, *19*, 3963−3972.

(10) Schröder, C.; Ren, J.; Rodrigues, A. C. M.; Eckert, H. Glass-to-Crystal Transition in $Li_{1+X}Al_XGe_{2-X}(PO_4)_3$: Structural Aspects Studied by Solid State NMR. *J. Phys. Chem. C* **2014**, *118*, 9400−9411.

(11) Yu, S.; Schmidt, R. D.; Garcia-Mendez, R.; Herbert, E.; Dudney, N. J.; Wolfenstine, J. B.; Sakamoto, J.; Siegel, D. J. Elastic Properties of the Solid Electrolyte $Li_7La_3Zr_2O_{12}$ (LLZO). *Chem. Mater.* **2016**, *28*, 197−206.

(12) Wang, Z. Q.; Wu, M. S.; Liu, G.; Lei, X. L.; Xu, B.; Ouyang, C. Y. Elastic Properties of New Solid State Electrolyte Material Li10GeP2S12: A Study from First-Principles Calculations. *Int. J. Electrochem. Sci.* **2014**, *9*, 562−568.

(13) Xue, Z.; He, D.; Xie, X. Poly(ethylene Oxide)-Based Electrolytes for Lithium-Ion Batteries. *J. Mater. Chem. A* **2015**, *3*, 19218−19253.

(14) Duan, H.; Yin, Y.-X; Zeng, X.-X; Li, J.-Y; Shi, J.-L; Shi, Y.; Wen, R.; Guo, Y.-G.; Wan, L.-J In-Situ Plasticized Polymer Electrolyte with Double-Network for Flexible Solid-State Lithium-Metal Batteries. *Energy Storage Mater.* **2018**, *10*, 85−91.

(15) Zeng, X.-X; Yin, Y.-X; Li, N.-W.; Du, W.-C.; Guo, Y.-G; Wan, L.-J Reshaping Lithium Plating/Stripping Behavior via Bifunctional Polymer Electrolyte for Room-Temperature Solid Li Metal Batteries. *J. Am. Chem. Soc.* **2016**, *138*, 15825−15828.

(16) Appetecchi, G. B.; Croce, F.; Hassoun, J.; Scrosati, B.; Salomon, M.; Cassel, F. Hot-Pressed, Dry, Composite, PEO-Based Electrolyte Membranes: I. Ionic Conductivity Characterization. *J. Power Sources* **2003**, *114*, 105−112.

(17) Cho, T.-H.; Tanaka, M.; Onishi, H.; Kondo, Y.; Nakamura, T.; Yamazaki, H.; Tanase, S.; Sakai, T. Battery Performances and Thermal Stability of Polyacrylonitrile Nano-Fiber-Based Nonwoven Separators for Li-Ion Battery. *J. Power Sources* **2008**, *181*, 155−160.

(18) Chen, H.-W.; Lin, T.-P.; Chang, F.-C. Ionic Conductivity Enhancement of the Plasticized PMMA/LiClO 4 Polymer Nanocomposite Electrolyte Containing Clay. *Polymer* **2002**, *43*, 5281−5288.

(19) Chen, R.; Qu, W.; Guo, X.; Li, L.; Wu, F. The Pursuit of Solid-State Electrolytes for Lithium Batteries: From Comprehensive Insight to Emerging Horizons. *Mater. Horiz.* **2016**, *3*, 487−516.

(20) Marcinek, M.; Bac, A.; Lipka, P.; Zalewska, A.; Żukowska, G.; Borkowska, R.; Wieczorek, W. Effect of Filler Surface Group on Ionic Interactions in PEG-$LiClO_4$ -Al_2O_3 Composite Polyether Electrolytes. *J. Phys. Chem. B* **2000**, *104*, 11088−11093.

(21) Scrosati, B.; Croce, F.; Persi, L. Impedance Spectroscopy Study of PEO-Based Nanocomposite Polymer Electrolytes. *J. Electrochem. Soc.* **2000**, *147*, 1718−1721.

(22) Xue, Z.; He, D.; Xie, X. Poly(ethylene Oxide)-Based Electrolytes for Lithium-Ion Batteries. *J. Mater. Chem. A* **2015**, *3*, 19218−19253.

(23) Ahn, J.-H.; Wang, G. X.; Liu, H. K.; Dou, S. X. Nanoparticle-Dispersed PEO Polymer Electrolytes for Li Batteries. *J. Power Sources* **2003**, *119*−*121*, 422−426.

(24) Manuel Stephan, A.; Nahm, K. S. Review on Composite Polymer Electrolytes for Lithium Batteries. *Polymer* **2006**, *47*, 5952−5964.

(25) Kalnaus, S.; Tenhaeff, W. E.; Sakamoto, J.; Sabau, A. S.; Daniel, C.; Dudney, N. J. Analysis of Composite Electrolytes with Sintered Reinforcement Structure for Energy Storage Applications. *J. Power Sources* **2013**, *241*, 178−185.

(26) Fu, K. K.; Gong, Y.; Dai, J.; Gong, A.; Han, X.; Yao, Y.; Wang, C.; Wang, Y.; Chen, Y.; Yan, C.; Li, Y.; Wachsman, E. D.; Hu, L. Flexible, Solid-State, Ion-Conducting Membrane with 3D Garnet Nanofiber Networks for Lithium Batteries. *Proc. Natl. Acad. Sci. U.S.A.* **2016**, *113*, 7094−7099.

(27) Villaluenga, I.; Wujcik, K. H.; Tong, W.; Devaux, D.; Wong, D. H. C.; DeSimone, J. M.; Balsara, N. P. Compliant Glass-polymer Hybrid Single Ion-Conducting Electrolytes for Lithium Batteries. *Proc. Natl. Acad. Sci. U.S.A.* **2016**, *113*, 52−57.

(28) Liu, W.; Liu, N.; Sun, J.; Hsu, P.-C.; Li, Y.; Lee, H.-W.; Cui, Y. Ionic Conductivity Enhancement of Polymer Electrolytes with Ceramic Nanowire Fillers. *Nano Lett.* **2015**, *15*, 2740−2745.

(29) Jung, Y.-C.; Lee, S.-M.; Choi, J.-H.; Jang, S. S.; Kim, D.-W. All Solid-State Lithium Batteries Assembled with Hybrid Solid Electrolytes. *J. Electrochem. Soc.* **2015**, *162*, A704−A710.

(30) Zheng, J.; Tang, M.; Hu, Y.-Y. Lithium Ion Pathway within $Li_7La_3Zr_2O_{12}$ -Polyethylene Oxide Composite Electrolytes. *Angew. Chem., Int. Ed.* **2016**, *55*, 12538−12542.

(31) Yang, T.; Zheng, J.; Cheng, Q.; Hu, Y.-Y.; Chan, C. K. Composite Polymer Electrolytes with $Li_7La_3Zr_2O_{12}$ Garnet-Type Nanowires as Ceramic Fillers: Mechanism of Conductivity Enhance-

DOI: 10.1021/acsami.7b17301
ACS Appl. Mater. Interfaces 2018, 10, 4113−4120

ment and Role of Doping and Morphology. *ACS Appl. Mater. Interfaces* **2017**, *9*, 21773−21780.
(32) Zheng, J.; Dang, H.; Feng, X.; Chien, P.-H.; Hu, Y.-Y. Li-Ion Transport in a Representative Ceramic-polymer-plasticizer Composite Electrolyte: $Li_7La_3Zr_2O_{12}$ -polyethylene Oxide-tetraethylene Glycol Dimethyl Ether. *J. Mater. Chem. A* **2017**, *5*, 18457−18463.
(33) Bandyopadhyay, S.; Marzke, R. F.; Singh, R. K.; Newman, N. Electrical Conductivities and Li Ion Concentration-Dependent Diffusivities, in Polyurethane Polymers Doped with Lithium Trifluoromethanesulfonimide (LiTFSI) or Lithium Perchlorate (LiClO4). *Solid State Ionics* **2010**, *181*, 1727−1731.
(34) Lee, H.; Yanilmaz, M.; Toprakci, O.; Fu, K.; Zhang, X. A Review of Recent Developments in Membrane Separators for Rechargeable Lithium-Ion Batteries. *Energy Environ. Sci.* **2014**, *7*, 3857−3886.
(35) Huo, H.; Zhao, N.; Sun, J.; Du, F.; Li, Y.; Guo, X. Composite Electrolytes of Polyethylene Oxides/Garnets Interfacially Wetted by Ionic Liquid for Room-Temperature Solid-State Lithium Battery. *J. Power Sources* **2017**, *372*, 1−7.

DOI: 10.1021/acsami.7b17301
ACS Appl. Mater. Interfaces 2018, 10, 4113−4120